Electronic Supplementary Material (ESI) for Materials Advances.
This journal is © The Royal Society of Chemistry 2021

SUPPORTING INFORMATION

Regulation of bi-color fluorescence changes of AIE supramolecular self-assembly gels by the interaction with Al^{3+} and energy transfer

Xinxian Ma*[a], Jinlong Yue[#a], Bo Qiao[a], Lili Zhou[a], Yang Gao[a], Yipei Wang[a], Yingshan Lai[a], Yutao Geng[a], Enke Feng[a], Minghua Liu*[b]

College of Chemistry and Chemical Engineering, Ningxia Normal University, Guyuan 756000, People's Republic of China.Fax: 86 954 2079637; Tel: 86 954 2079637; E-mail: maxinxian@163.com

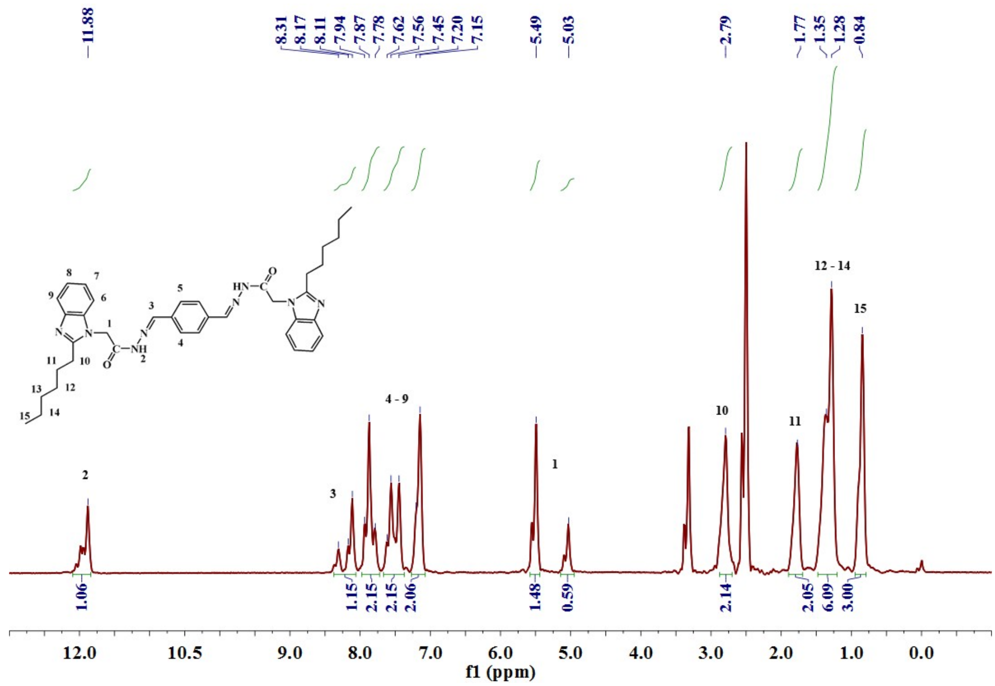

Fig. S1. ^{1}H NMR spectrum of **BD** in DMSO-d_6

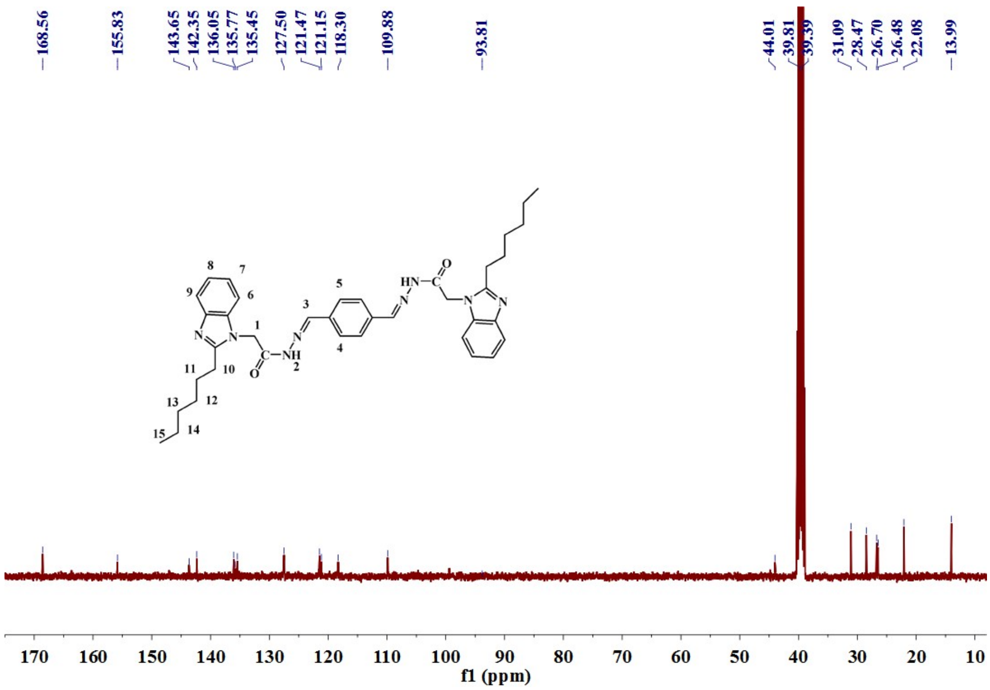

Fig. S2. ^{13}C NMR spectrum of **BD** in DMSO-d_6

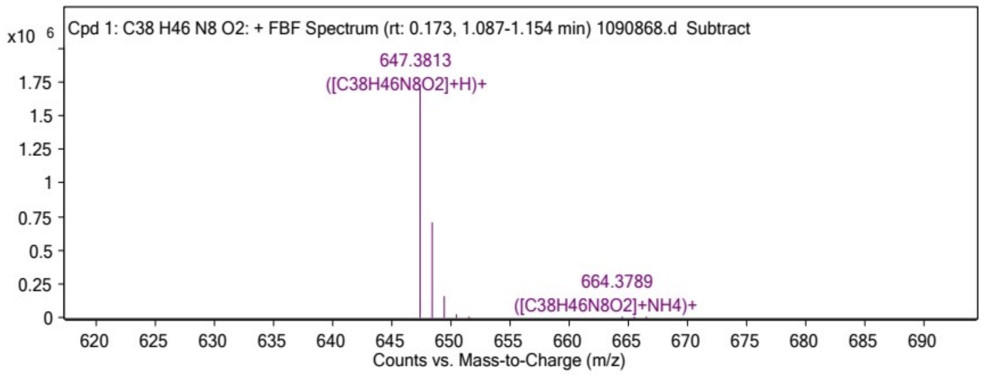

Fig. S3. ESI-MS spectrum of **BD**

Table S1 Gelation properties of the supramolecular gel **BDG**

Entry	**Solvent**	**State**[a]	**CGC**[b](%)	**T_{gel}**[c] (°C, wt %)
1	water	P	\	\
2	cyclohexane	P	\	\
3	petroleum ether	P	\	\
4	THF	P	\	\
5	$CHCl_3$	P	\	\
6	CH_2Cl_2	P	\	\
7	acetone	P	\	\
8	DMF	G	2.5	74(2.5%)
9	DMF-H_2O	G	0.5	95(0.5%)
10	DMSO	G	2	82(2%)
11	DMSO-H_2O	G	0.5	102(0.5%)
12	methanol	P	\	\
13	ethanol	S	\	\
14	ethanol-H_2O	P	\	\
15	ethanediol	P	\	\
16	isopropanol	P	\	\
17	n-butyl alcohol	P	\	\
18	n-amyl alcohol	P	\	\
19	isopentanol	P	\	\
20	n-hexanol	P	\	\
21	ethyl acetate	P	\	\
22	acetonitrile	P	\	\
23	CCl_4	P	\	\

[a] G, P and S denote gelation, precipitation and solution, respectively

[b] The critical gelation concentration (wt %, 10 mg/mL = 1.0%)

[c] The gelation temperature (°C)

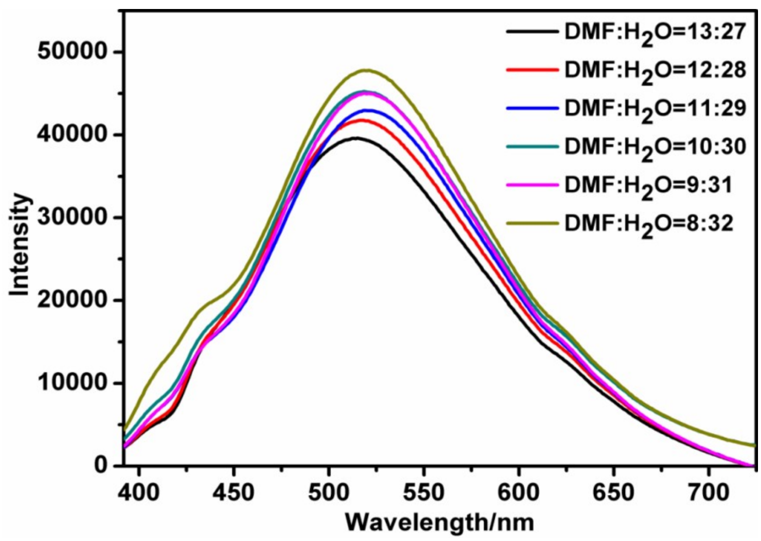

Fig. S4. fluorescent spectra of BDG with different water content

(0.5%, λ_{ex} = 372 nm)

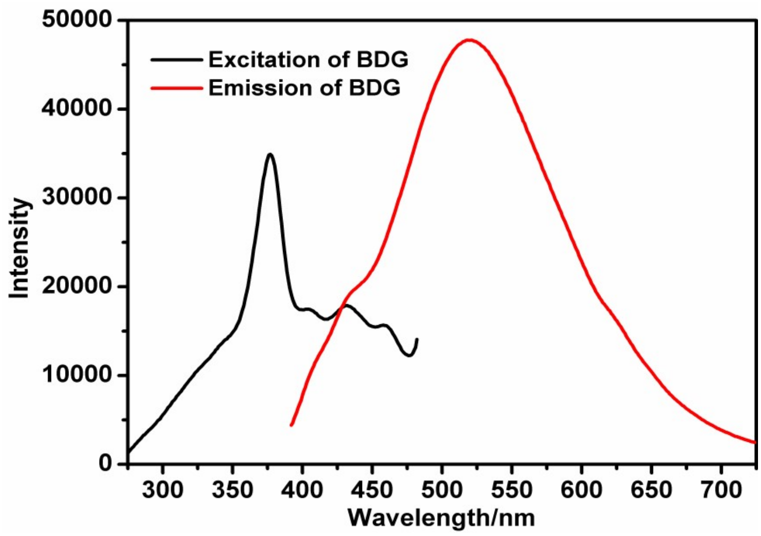

Fig. S5. Excitation spectrum and emission spectrum of BDG (0.5%, V_{DMF} : V_{water} = 1 : 4)

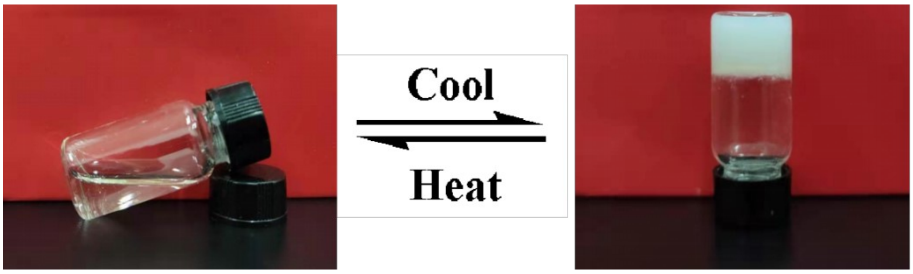

Fig. S6. Illustration for reversible gel-sol transformation of the BDG triggered by temperature (0.5%, V_{DMSO} : V_{water} = 1 : 4)

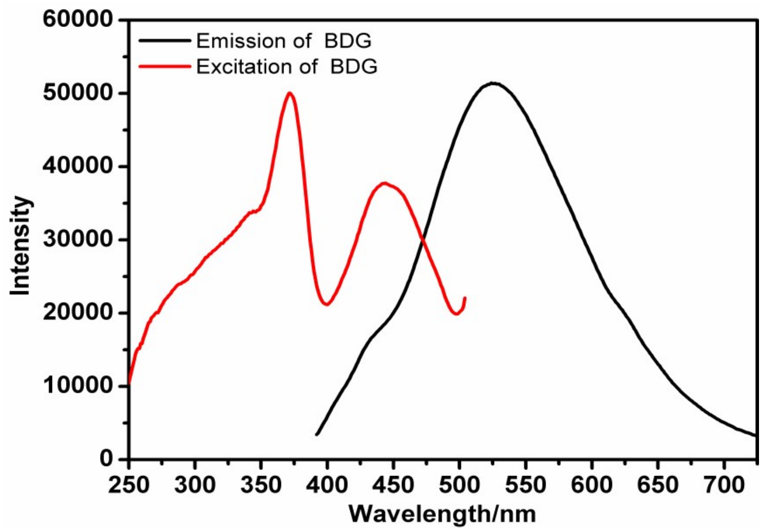

Fig. S7. Excitation spectrum and emission spectrum of BDG (0.5%, $V_{DMSO} : V_{water} = 1 : 4$)

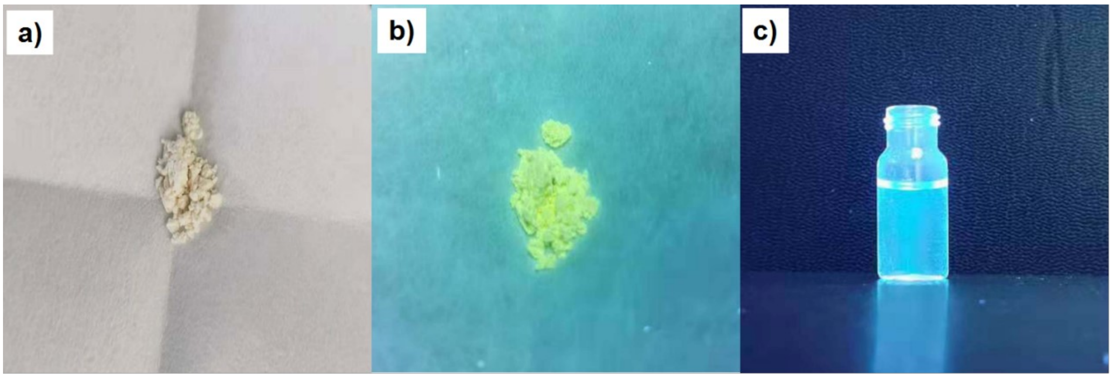

Fig. S8. The photos of BD powder (25 °C) were taken under a) daylight and b) UV light, respectively. c) The photo of BD in DMF (1×10^{-4} M, 25°C) were taken under UV light

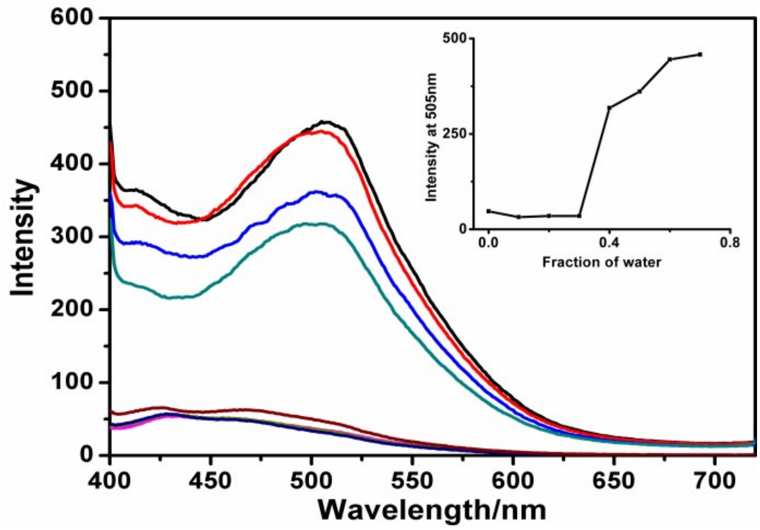

Fig. S9. Fluorescence spectra of BD (3×10^{-4} M) in a DMF/H_2O mixed solution at different vol % (λ_{ex} = 372 nm). Inset: Fluorescence intensity of BD at 505 nm in the presence of different faction of water from 0 to 70%

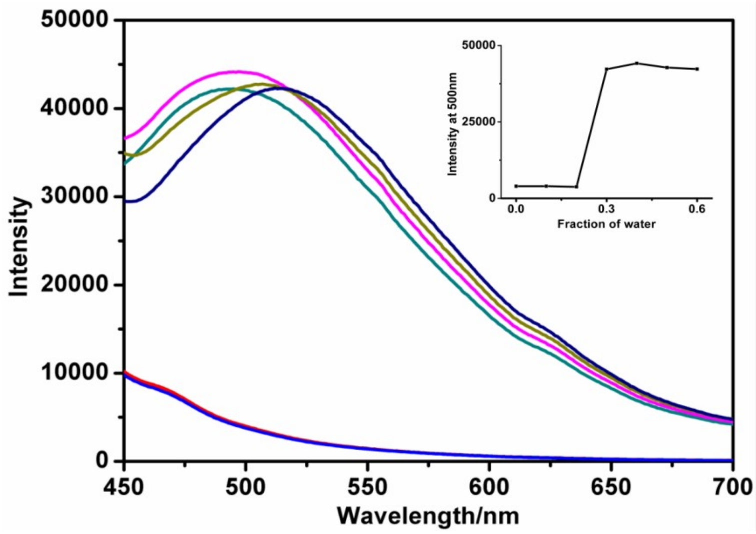

Fig. S10. Fluorescence spectra of BD (3×10^{-4} M) in a DMSO/H_2O mixed solution at different vol % (λ_{ex} = 372 nm). Inset: Fluorescence intensity of BD at 510 nm in the presence of different faction of water from 0 to 60%

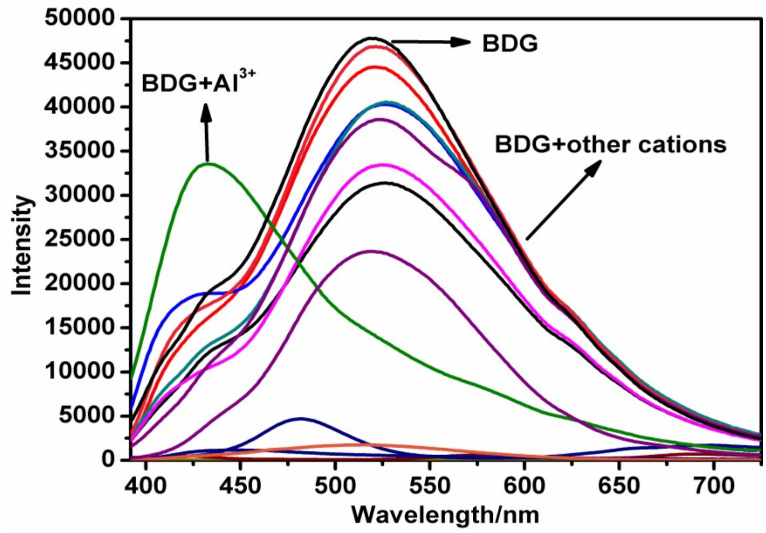

Fig. S11. Fluorescence spectra (λ_{ex} = 372 nm) of BDG (0.5%, V_{DMF} : V_{water} = 1 : 4) in the presence of various cations (10.0 equiv.). Respectively, using 0.1 M nitrate solution as the sources at room temperature

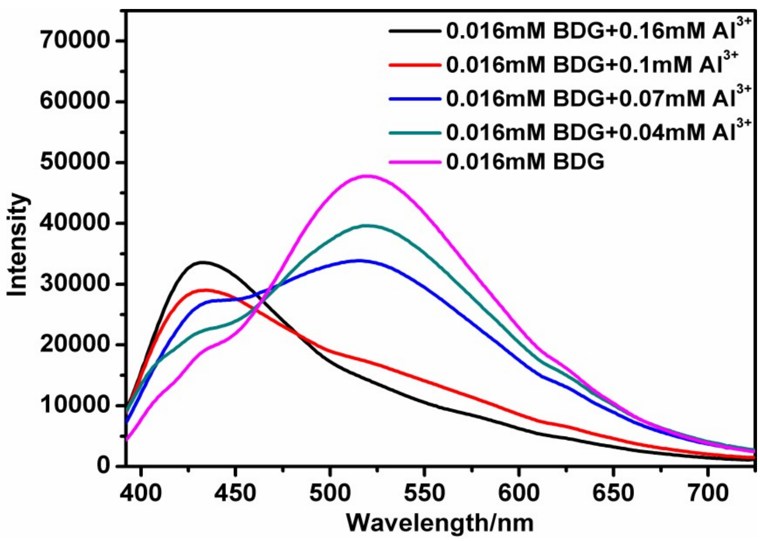

Fig. S12. Fluorescent titration spectra (λ_{ex} = 372 nm) of BDG (7.7 mM) upon addition of Al^{3+} in DMF/H_2O (V_{DMF} : V_{water} =1 : 4)

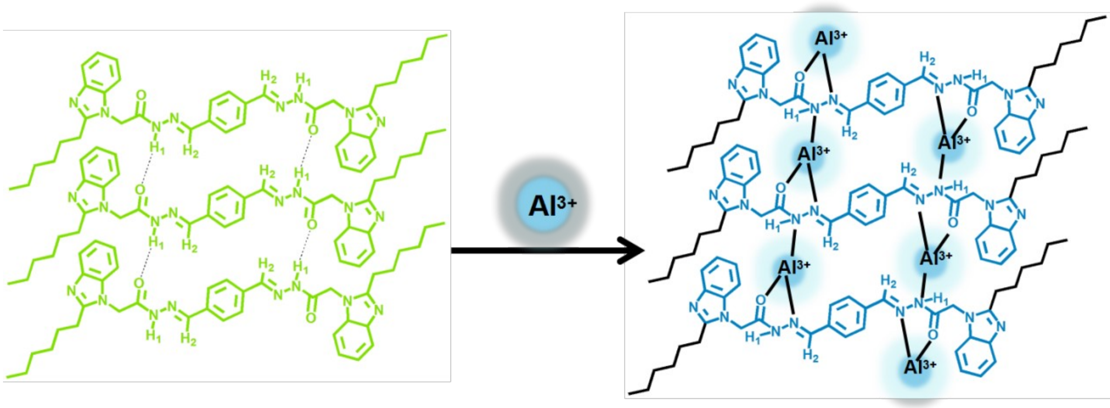

Fig. S13. Proposed sensing mechanism of BDG for Al^{3+}

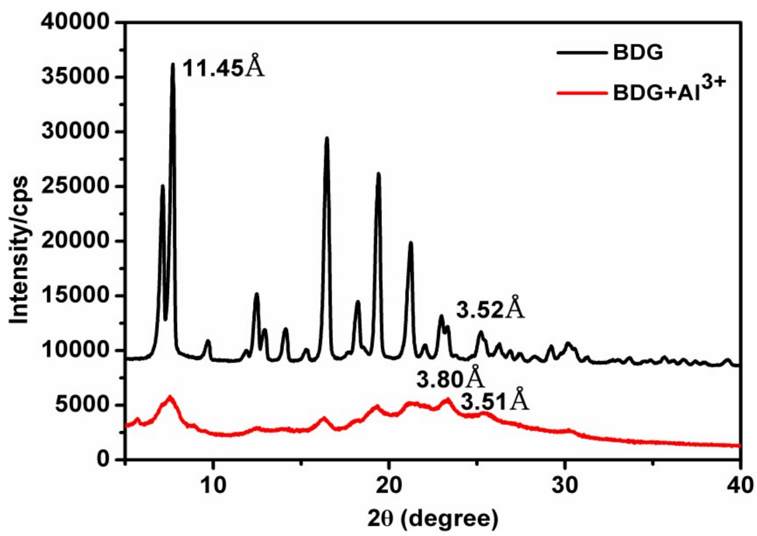

Fig. S14. The powder X-ray diffraction pattern of the xerogel BDG and BDG-Al

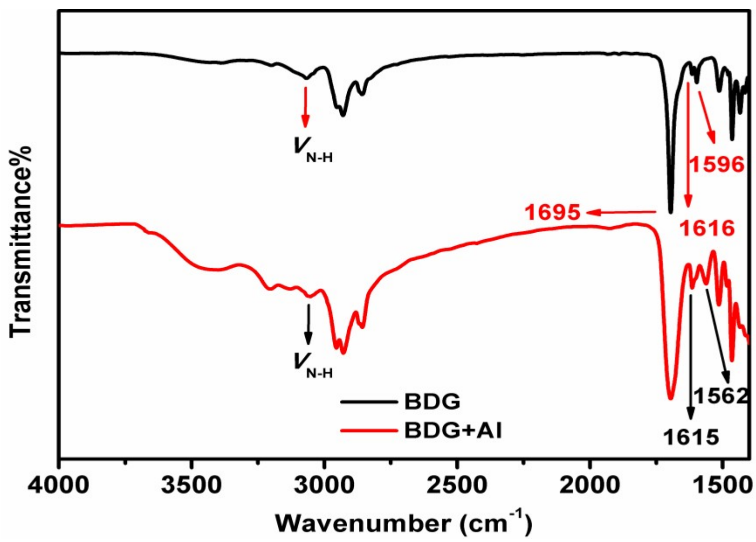

Fig. S15. FT-IR spectra of the xerogel BDG and BDG-Al

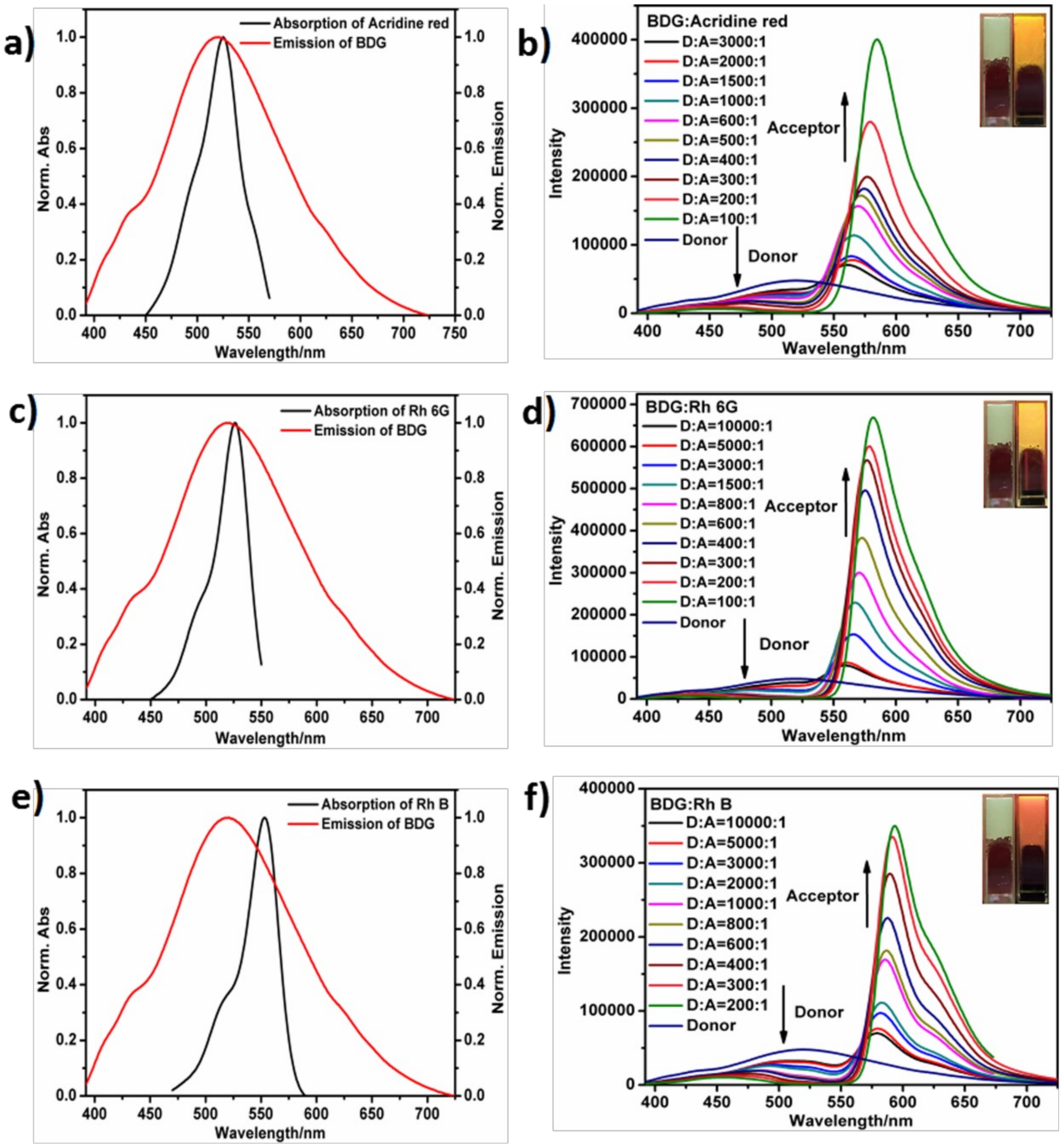

Fig. S16. Normalized emission spectrum of BDG (7.7 mM), absorption spectrum of (a) Acridine red (1×10^{-5} M), (c) Rh B (1×10^{-5} M) and (e) Rh 6G (1×10^{-5} M). Fluorescence spectra of BDG (7.7 mM) in gel with different concentrations of (b) Acridine red (77 μM, λ_{ex} = 372 nm, Inset: photographs of BDG, BDG/acridine red), (d) Rh 6G (77 μM, λ_{ex} = 372 nm, Inset: photographs of BDG, BDG/Rh 6G) and (f) Rh B (38.5 μM, λ_{ex} = 372 nm, Inset: photographs of BDG, BDG/Rh B under UV light)

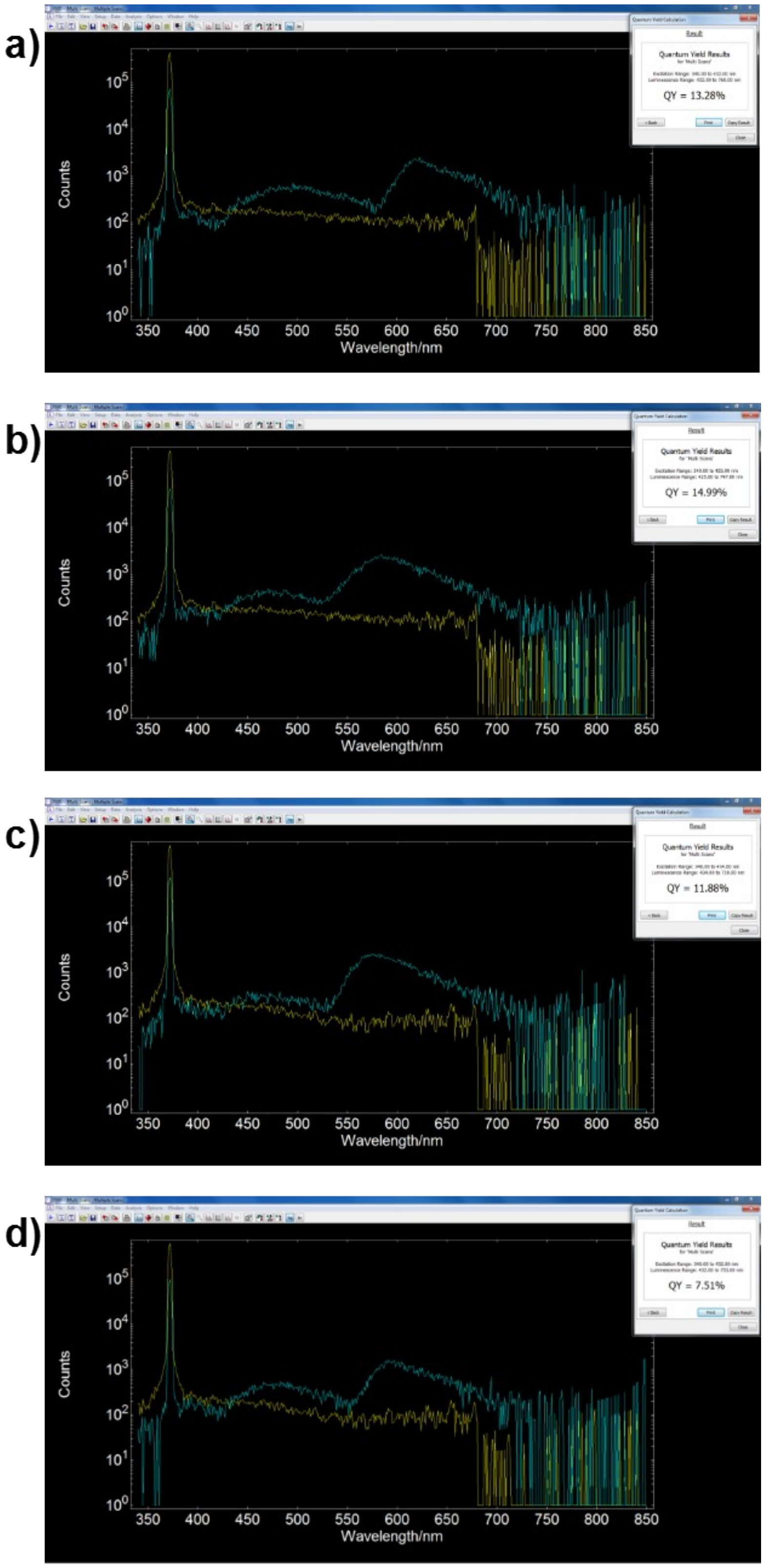

Fig. S17. Absolute fluorescence quantum yields ($\Phi_{f(abs)}$) of (a) BDG / SR 101 (7.7 mM / 38.5 mM), (b) BDG / acridine red (7.7 mM / 77 μM), (c) BDG / Rh 6G (7.7 mM / 77 μM) and (d) BDG / Rh B (7.7 mM / 38.5 μM) (λ_{ex} = 372 nm) in DMF/H_2O

Energy-transfer efficiency, Φ_{ET}, the fraction of the absorbed energy that is transferred to the acceptor is experimentally measured as a ratio of the fluorescence intensities of the donor in the absence and presence of the acceptor (I_D and I_{DA}).[1]

$$\Phi_{ET}=1-I_{DA}/I_D$$

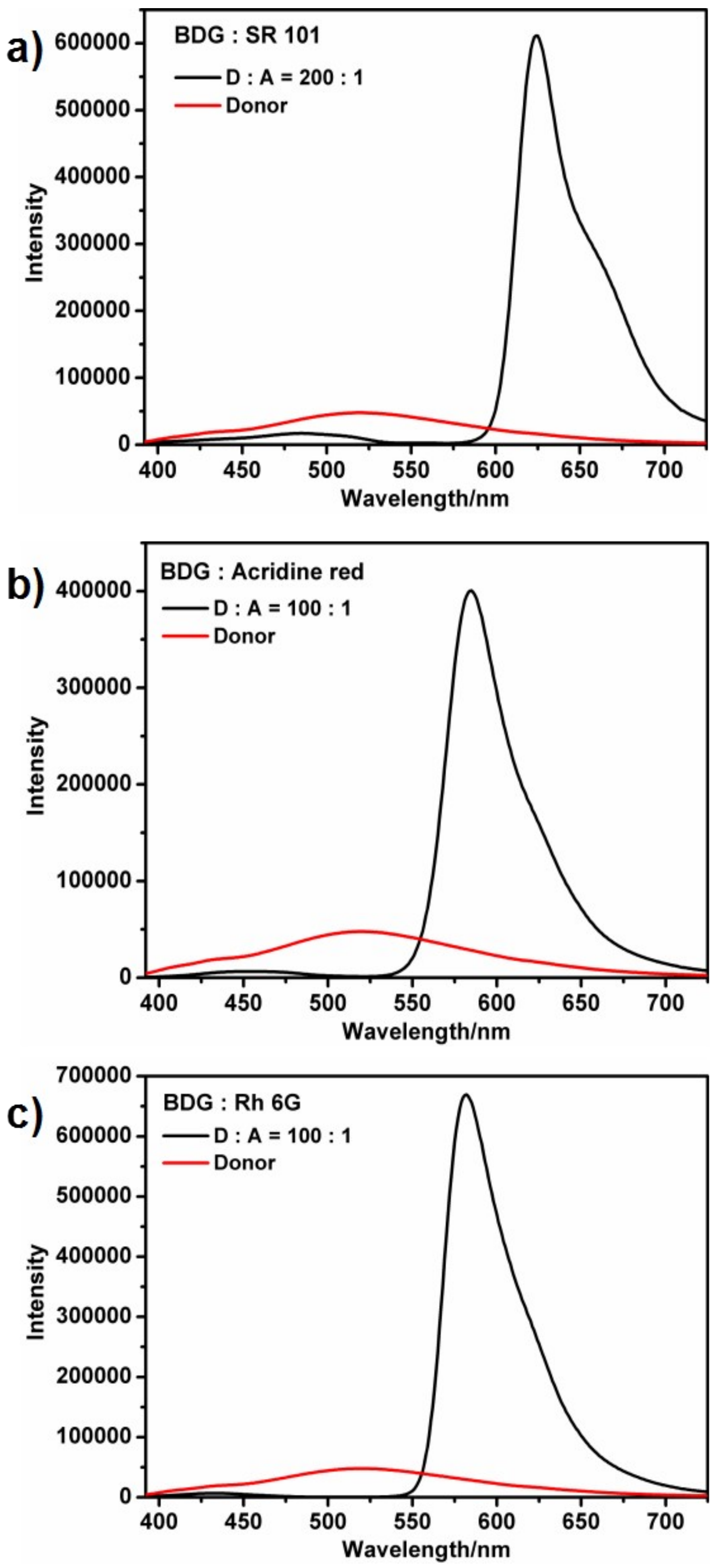

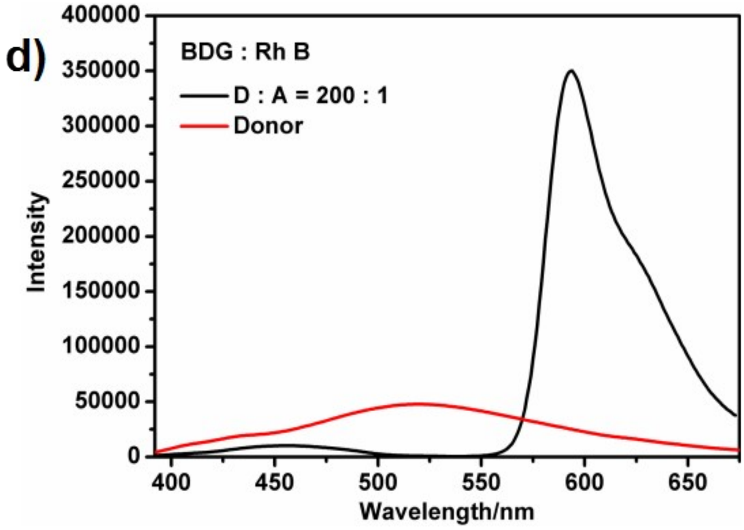

Fig. S18. Fluorescence spectra of a) BDG and BDG/SR 101 assembly, b) BDG and BDG/acridine red assembly, c) BDG and BDG/Rh 6G assembly and d) BDG and BDG/Rh B assembly (λ_{ex} = 372 nm, [BDG] = 7.7 mM, [SR 101] = 38.5 μM, [acridine red] = 77 μM, [Rh 6G] = 77 μM and [Rh B] = 38.5 μM)

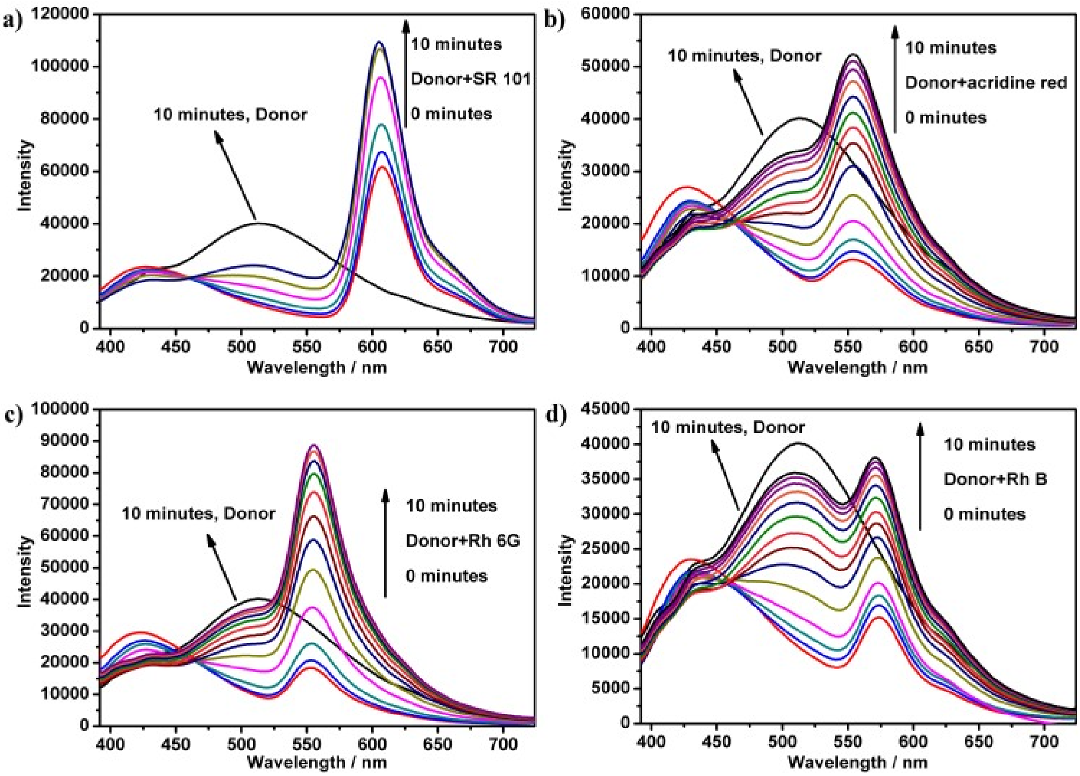

Fig. S19. Fluorescence spectra (λ_{ex} = 372 nm) of a) BDG and BDG/SR 101, b) BDG/acridine red, c) BDG/Rh 6G and d) BDG/Rh B in mixed solutions ([BDG] = 2.5 mM, [SR 101] = 0.83 μM, [acridine red] = 0.83 μM, [Rh 6G] = 0.25 μM and [Rh B] = 0.25 μM, $V_{DMF} : V_{water}$ = 1 : 4)

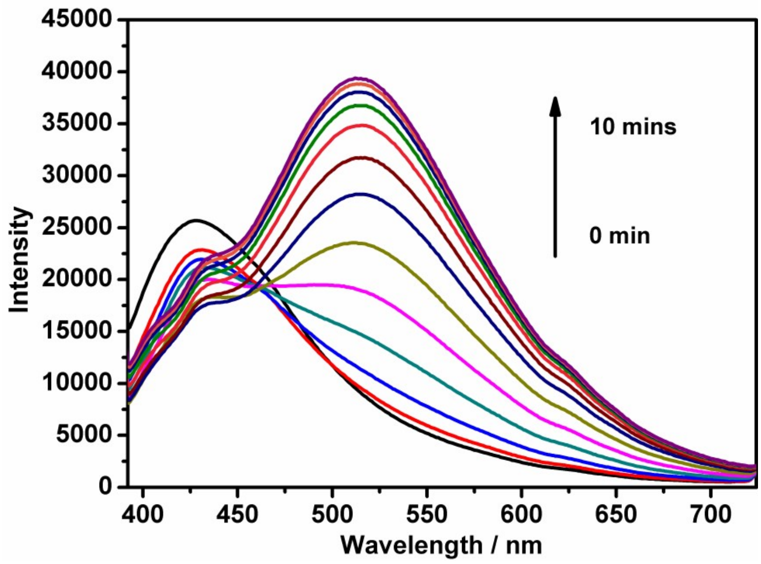

Fig. S20. Fluorescence spectra (λ_{ex} = 372 nm) of BD during the gelation process from 95 °C to 25 °C ([BD] = 2.5 mM, V_{DMF} : V_{water} =1 : 4)

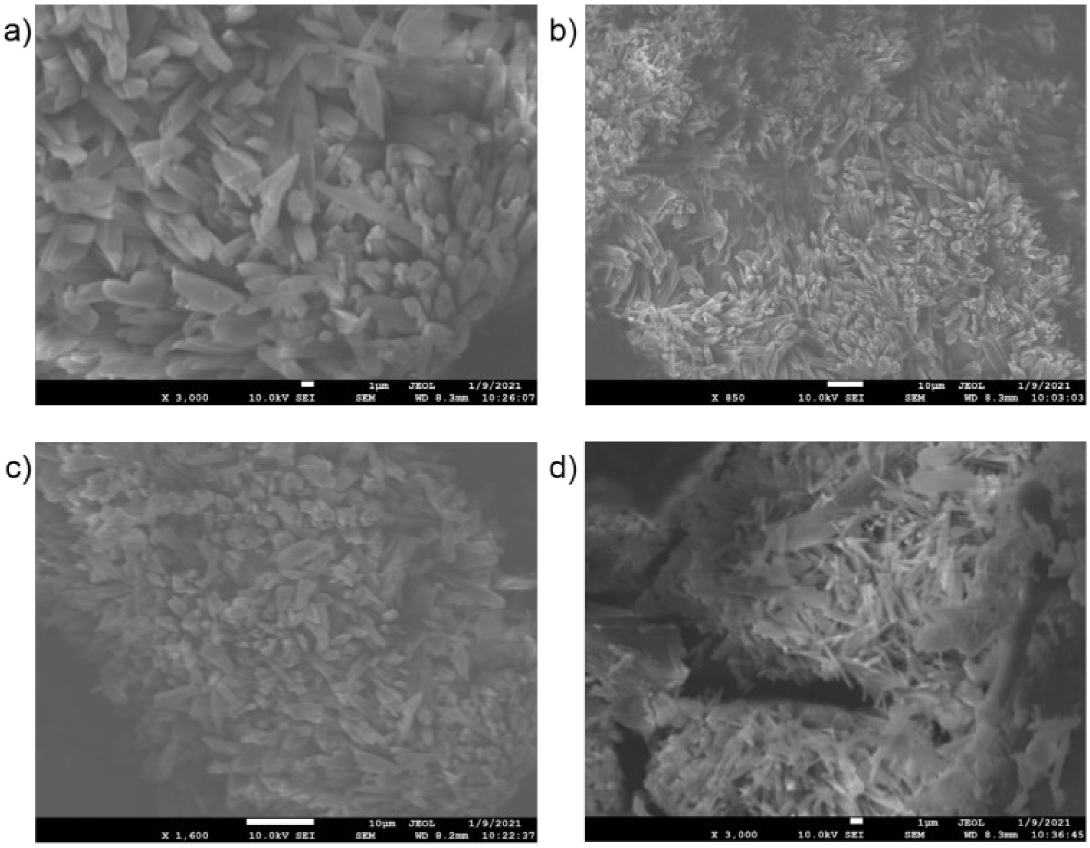

Fig. S21. FE-SEM micrographs of the xerogel of a) BDG/SR 101, b) BDG/acridine red, c) BDG/Rh 6G and d) BDG/Rh B. The gel was two days old before the images were taken. ([BDG] = 7.7 mM, [SR 101] = 38.5 μM, [acridine red] = 77 μM, [Rh 6G] = 77 μM and [Rh B] = 38.5 μM, $V_{DMF} : V_{water} = 1 : 4$)

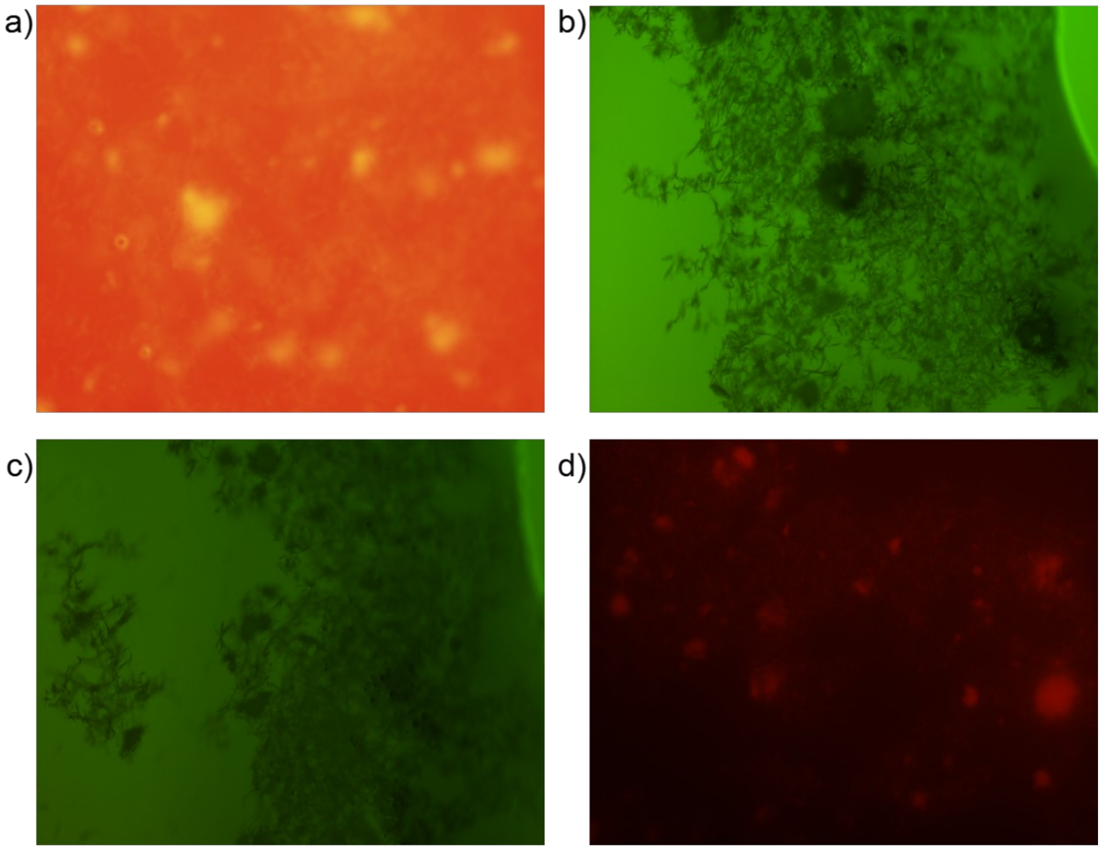

Fig. S22. FOM images of a) BDG/SR 101, b) BDG/acridine red, c) BDG/Rh 6G and d) BDG/Rh B. ([BDG] = 7.7 mM, [SR 101] = 38.5 μM, [acridine red] = 77 μM, [Rh 6G] = 77 μM and [Rh B] = 38.5 μM, $V_{DMF} : V_{water} = 1 : 4$)

1. (a) J. J. Li, Y. Chen, J. Yu, N. Cheng and Y. Liu, Adv. Mater., 2017, **29**, 1701905-1701909; (b) S. Guo, Y. Song, Y. He, X. Y. Hu and L. Y. Wang, Angew. Chem. Int. Ed., 2018, **57**, 3163-3167; (c) M. Hao, G. P. Sun, M. Z. Zuo, Z. Q. Xu, Y. Chen, X. Y. Hu and L. Y. Wang, Angew. Chem. Int. Ed., 2020, **59**, 10095-10100.